

Optimum End-to-End Distortion of Interleaved Transmission via a Rayleigh MIMO Channel

Jinhui Chen and Dirk T. M. Slock
Eurecom
Sophia Antipolis, France
Email: {jin-hui.chen, dirk.slock}@eurecom.fr

Abstract—¹ In this paper, we study the optimum expected end-to-end distortion on a reproduced white thermal noise source conveyed over a flat Rayleigh fading multi-input multi-output (MIMO) channel with time-interleaving. Assuming no outage event happens, perfect channel information at the receiver and ideal interleaving, we derive the analytical expression of the tight lower bound on the expected quadratic end-to-end distortion for general signal-to-noise ratios (SNR) and analyze its asymptotic form at high SNR. Straightforwardly, the tight lower bound for no-outage cases is also a lower bound for outage cases although loose. Our results expose the mechanism of how time diversity branches benefit the end-to-end distortion for a MIMO system.

I. INTRODUCTION

For a time-variant fading channel, it is very well-known that interleaving techniques can be used to exploit the time diversity and thereby benefits error probability [1]. For single-input single-output (SISO) channels, the symbol-by-symbol (see [2], [3], etc.) and bit-by-bit (see [4] etc.) interleavers for separate source-channel coding have been being developed for many years. In [5], The performance of the symbol-by-symbol interleavers is analyzed with respect to cut-off rate, channel capacity and the bounds of bit-error probability. In [6], Caire et al. not only analyze the performance of bit-interleaved coded modulation (BICM) for separate coding over SISO channels with respect to cut-off rate, channel capacity and the bounds of bit-error probability, but also propose the design criteria for BICM. Subsequently, an analysis of accurate error probability of BICM is provided in [7]. If readers would like to know more publications about interleaving for SISO channels, in [8], Biglieri et al. give a complete overview of interleaving techniques among all remarkable contributions for SISO fading channels by 1998. Of course, interleaving techniques can also be employed for joint source-channel coding (e.g., [9]) and MIMO channels (e.g., [10]).

To the best of our knowledge, most interest of analyzing system performance with time-interleaving has been mainly focused on the improvement of error probability and cutoff rate by exploiting multiple time diversity branches. Baltersee et al. analyze the achievable rates of MIMO channels with data-aided channel estimation and ideal interleaving in [11],

¹Eurecom's research is partially supported by its industrial members: BMW Group Research & Technology, Bouygues Telecom, Cisco, Hitachi, ORANGE, SFR, Sharp, STMicroelectronics, Swisscom, Thales. The work presented in this paper has also been partially supported by the European FP7 project Newcom++ and by the French ANR project Apogee.

where they suppose perfect interleaving to construct effective memoryless channels for source data part while training data for channel information at the receiver suffers from Doppler spread. So far, the effect of time diversity on reproduced analog (amplitude-continuous) source have not been studied. In practice, an analog source, such as voice, is to be separate or joint source-channel coded, interleaved and then transmitted in frames to whose lengths coding and decoding are subject. The frame length can be designed to be multiple of channel coherence time to exploit the time diversity. Obviously, to be in time and tractable, the frame length cannot be infinite, and thereby the number of time diversity branches to be exploited is limited. The mechanism of how the time interleaving benefits on reproducing an analog source in length-limited frames is of our interest in this paper.

For studying the reconstruction of an analog source, expected end-to-end distortion is the primary criterion. The relation between the quadratic end-to-end distortion (mean square error) and the channel capacity has been pointed out by Shannon in [12]. The *distortion exponent* of expected distortion [13] implied by Shannon's inequality,

$$\Delta = - \lim_{SNR \rightarrow \infty} \frac{\log \mathbb{E}[D]}{\log SNR}, \quad (1)$$

is studied in [13]–[16] and so on. An upper bound on Δ with respect to *the ratio of source bandwidth to channel bandwidth* (SCBR), has been derived in [15] and [16], respectively, by similar means to [17]. The settings in [15] and [16] are block-fading MIMO systems, time diversity being not exploited. They also provide schemes for achieving the upper bound of distortion exponent for a certain range of SCBR and antenna numbers.

More than what have been exposed by others, if we take a look at the asymptotic complete form of the lower bound of $\mathbb{E}[D]$ at high SNR,

$$ED^{LB} \sim \mu^* SNR^{-\Delta^{UB}} \quad (2)$$

where the *distortion factor* μ^* satisfies

$$\lim_{SNR \rightarrow \infty} \frac{\log \mu^*}{\log SNR} = 0, \quad (3)$$

we would have interest in the behavior of μ^* with antenna numbers and SCBR. This is what we have studied in [18], where we give the analytical expression of the lower bound of

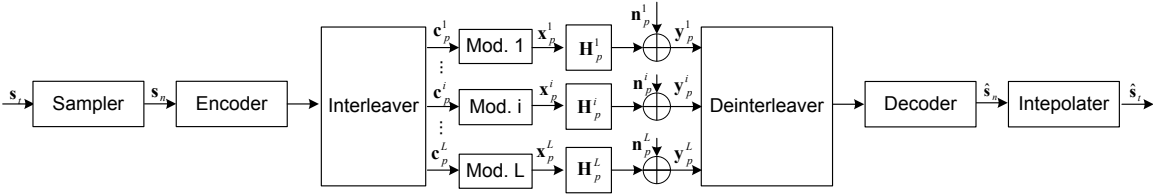


Fig. 1. Block diagram of the transmission model with perfect interleaving

expected distortion, thereby provide the same upper bound of the distortion exponent Δ^{UB} as in [15] [16] and the meaningful analytical expression of the corresponding distortion factor μ^* .

In this paper, considering ideal interleaving inside a length-limited frame over a noncoherent channel is just like separating sources to transmit via several parallel independent coherent channels, we develop our results in [18] to interleaving cases and illustrate how the time diversity works on the expected end-to-end distortion.

Note that just before the publication of this paper, we notice Gündüz and Erkip have obtained the same result in [19] as Theorem 2 in this paper, which is a coincidence to us. Nevertheless, the main targets of [19] and this paper are different. We focus more on the effect of interleaving. The most interesting part is the cooperation of the distortion exponent and the factor.

The remainder of this paper is organized as follows. The system model for ideal interleaving frame transmission is described in Section II. The analytical expression of expected end-to-end distortion for general SNR can be seen in Section III. Section IV gives the upper bound of the distortion exponent and the analytical expression of the corresponding distortion coefficient for the asymptotic expected distortion at high SNR. The effect of utilizing time diversity branches is illustrated in Section V. Finally, Section VI concludes the contributions of this paper.

II. SYSTEM MODEL

Consider a frequency-flat Rayleigh fading MIMO channel of bandwidth W_c with M inputs and N outputs. Assuming there are L time diversity branches in one frame, with ideal interleaving, we can regard the noncoherent channel as L parallel statistically-independent memory-less coherent channels. Fig.1 is the block diagram of the transmission model. Suppose a white thermal noise source s_t of bandwidth W_s and average power P_s is to be conveyed. First, it is sampled (over Nyquist sampling rate) into a time-discrete source. After separate or joint source-channel coding with ideal interleaving, the transmission can be regarded as L source symbols to be transmitted over L parallel channels at time p simultaneously. For each equivalent coherent channel, the channel model is represented as

$$\mathbf{y}_p^i = \mathbf{H}_i \mathbf{x}_p^i + \mathbf{n}_p^i, \quad 1 \leq i \leq L. \quad (4)$$

where all elements of \mathbf{H}_i are i.i.d. $\mathcal{CN}(0, 1)$ random variables and all elements of \mathbf{n}_p^i are zero-mean i.i.d. complex random

variables with variance σ_n^2 . Suppose $\|\mathbf{x}_p^i\|_2^2 = P_t$, the average SNR at each receive antenna $\rho = P_t/\sigma_n^2$. At the receiver, after deinterleaving and decoding, the estimate of the time-discrete source, \hat{s}_n , is obtained. Finally, the analog source is reconstructed as \hat{s}_t via interpolation.

III. EXPECTED END-TO-END DISTORTION

After transmission and processing, the end-to-end distortion is measured by the mean square error D ,

$$D = \lim_{T \rightarrow \infty} \frac{1}{T} \int_0^T (\hat{s}(t) - s(t))^2 dt \quad (5)$$

where $s(t)$ is the real source at time t and $\hat{s}(t)$ is the reproduced real source at time t . The source rate with the distortion fidelity D [12]

$$R_s = W_s \log \frac{P_s}{D}. \quad (6)$$

Since the channel can be regarded as parallel channels as Fig.1 shows, for per channel use, the mutual information of the channel,

$$\begin{aligned} \mathcal{I} &= \frac{1}{L} \sum_{i=1}^L \mathcal{I}_i \\ &= \frac{1}{L} \sum_{i=1}^L \log \det(\mathbf{I}_N + \frac{\rho}{M} \mathbf{H}_i \mathbf{H}_i^\dagger) \end{aligned} \quad (7)$$

where \mathbf{I}_N is the $N \times N$ identity matrix and \mathcal{I}_i is the mutual information per channel use for the i -th channel in the equivalent parallel channel bank.

We suppose no outage happen in the MIMO system, e.g., instantaneous channel rates are fed back as scalars and used to do joint source-channel coding. Assuming the channel is used at $2W_c$ channel uses per second as a time-discrete channel [20, pp. 248], according to Shannon's inequality [12], we obtain

$$W_s \log \frac{P_s}{D} \leq \frac{2W_c}{L} \sum_{i=1}^L \log \det(\mathbf{I}_N + \frac{\rho}{M} \mathbf{H}_i \mathbf{H}_i^\dagger). \quad (8)$$

Consequently,

$$D \geq P_s \prod_{i=1}^L \det(\mathbf{I}_N + \frac{\rho}{M} \mathbf{H}_i \mathbf{H}_i^\dagger)^{-\frac{2}{L\eta}}, \quad (9)$$

and thereby (10)

$$\mathbb{E}(D) \geq P_s \mathbb{E}_{\mathbf{H}} \left[\det(\mathbf{I}_N + \frac{\rho}{M} \mathbf{H} \mathbf{H}^\dagger)^{-\frac{2}{L\eta}} \right], \quad (11)$$

where η is the ratio of source bandwidth to channel bandwidth (SCBR), W_s/W_c , and $\mathbb{E}_{\mathbf{H}}[\cdot]$ is the expectation with respect to the random channel matrix \mathbf{H} .

In [18], by using the mathematical results on moment generating function of the capacity of uncorrelated Rayleigh MIMO channels in [21], we derive the analytical expression of $\mathbb{E}^{LB}(D)$ for the case $L = 1$. Straightforwardly, we can derive the expression for arbitrary positive integer L as follows. The proof is omitted due to lack of space.

Theorem 1 (Expected quadratic distortion lower bound):

The expected quadratic distortion is lower bounded by

$$ED^{LB} = P_s \left(\frac{\det \mathbf{G}}{\prod_{k=1}^m \Gamma(n-k+1)\Gamma(m-k+1)} \right)^L \quad (14)$$

where $m = \min\{M, N\}$, $n = \max\{M, N\}$, and \mathbf{G} is a $m \times m$ Hankel matrix whose (i, j) -th entry is

$$g_{ij} = \left(\frac{\rho}{M} \right)^{-d_{ij}} \Gamma(d_{ij}) \Psi \left(d_{ij}, d_{ij} + 1 - \frac{2}{\eta L}; \frac{M}{\rho} \right), \quad (15)$$

where $d_{ij} = i + j + n - m - 1$, $1 \leq i, j \leq m$, and $\Psi(a, b; x)$ is the Ψ function in [22]. \square

IV. DISTORTION EXPONENT AND FACTOR

Observing the expression in Theorem 1, we can see that ED^{LB} is in the form of $\sum_i \mu_i \rho^{-\Delta_i}$. Therefore, at asymptotically high SNR, the approximate form of ED^{LB} is

$$ED^{LB} \sim \mu^* \rho^{-\Delta^{UB}} \quad (16)$$

where $\mu^* \rho^{-\Delta^{UB}}$ is the term of the highest-order in (14), the upper bound of the distortion exponent $\Delta^{UB} = \min\{\Delta_i\}$, and μ^* is the corresponding distortion factor. Following the derivation in [18], we can get analytical expressions of Δ^{UB} and μ^* as follows. The proofs are omitted due to lack of space.

Theorem 2 (Distortion exponent upper bound): At the asymptotically high SNR, the distortion exponent is upper bounded by

$$\Delta^{UB} = L \sum_{i=1}^m \min \left\{ \frac{2}{L\eta}, 2i - 1 + |M - N| \right\} \quad (17)$$

\square

Theorem 3 (Corresponding distortion factor): Define two functions $\kappa_l(\beta, t)$ and $\kappa_h(\beta, t)$ as (12) and (13) at the top of this page, for $\beta \in \mathbb{R}^+$ and $t \in \{0, \mathbb{Z}^+\}$.

μ^* is given as follows,

1. For $\frac{2}{\eta L} \in (0, n - m + 1)$, i.e., $\eta \in (\frac{2}{L(n-m+1)}, +\infty)$ (termed *high SCBR* in this paper), the corresponding distortion factor is

$$\mu^* = P_s M^{\Delta^{UB}} \left(\frac{\kappa_h(\frac{2}{\eta L}, m)}{\prod_{k=1}^m \Gamma(n-k+1)\Gamma(m-k+1)} \right)^L, \quad (18)$$

and monotonically decreasing with n .

And,

$$\Delta^{UB} = \frac{2m}{\eta}. \quad (19)$$

2. For $\frac{2}{\eta L} \in (n + m - 1, +\infty)$, i.e., $\eta \in (0, \frac{2}{L(n+m-1)})$ (termed *low SCBR*), the corresponding distortion factor is

$$\mu^* = P_s M^{\Delta^{UB}} \left(\frac{\kappa_l(\frac{2}{\eta L}, m)}{\prod_{k=1}^m \Gamma(n-k+1)\Gamma(m-k+1)} \right)^L. \quad (20)$$

And,

$$\Delta^{UB} = LMN. \quad (21)$$

3. For $\frac{2}{\eta L} \in [n - m + 1, n + m - 1]$, i.e., $\eta \in [\frac{2}{L(n+m-1)}, \frac{2}{L(n-m+1)}]$ (termed *moderate SCBR*), there are two cases: in the case that $\frac{2}{\eta L} - (n - m - 1)$ is not an even number, the corresponding distortion factor is

$$\mu^* = P_s M^{\Delta^{UB}} \left(\frac{\kappa_l(\frac{2}{\eta L}, l) \kappa_h(\frac{2}{\eta L} - 2l, m - l)}{\prod_{k=1}^m \Gamma(n-k+1)\Gamma(m-k+1)} \right)^L; \quad (22)$$

in case that $\frac{2}{\eta L} - (n - m - 1)$ is an even number, the corresponding distortion factor is

$$\mu^* = P_s M^{\Delta^{UB}} \log \left(\frac{\rho}{M} \right) \cdot \left(\frac{\kappa_l(\frac{2}{\eta L}, l - 1) \kappa_h(\frac{2}{\eta L} - 2l, m - l)}{\prod_{k=1}^m \Gamma(n-k+1)\Gamma(m-k+1)} \right)^L, \quad (23)$$

where $l = \lceil \frac{\frac{2}{\eta L} - (n - m - 1)}{2} \rceil$. And,

$$\Delta^{UB} = Ll(l + n - m) + \frac{2(m - l)}{\eta}. \quad (24)$$

Note that $\lceil x \rceil$ rounds x to the nearest integer towards minus infinity. \square

V. INTERLEAVING IMPACT ANALYSIS

In this section, we analyze the interleaving impact on end-to-end distortion. Our discussion is focused on the approximated optimal end-to-end distortion at high SNR.

The approximate ED^{LB} is denoted by ED^{LB*} ,

$$ED^{LB*} = \mu^* \rho^{-\Delta^{UB}}. \quad (25)$$

When the time diversity branches $L \leq \lceil \frac{2}{\eta(n-m+1)} \rceil$, i.e., $\eta \leq \frac{2}{L(n-m+1)}$, the system is at either the low SCBR or the moderate SCBR as Theorem 3 indicates. We can see that in both cases, Δ^{UB} increases with L , which leads ED^{LB*} to decrease with L in the high SNR regime.

Fig.2 shows the relevance between ED^{LB} and L at low SCBR. ED^{LB} 's in a logarithmic scale to SNR in decibel are figured out by generating 1 000 000 realizations of \mathbf{H} and evaluating the right hand side of (11). Lines are not very smooth due to the precision limit of MATLAB. From Fig.

$$\kappa_l(\beta, t) = \begin{cases} \Gamma(n-m+1) \frac{\Gamma(\beta-n+m-1)}{\Gamma(\beta)} \prod_{k=2}^t \Gamma(k) \Gamma(n-m+k) \frac{\Gamma(\beta-n+m-2k+2) \Gamma(\beta-n+m-2k+1)}{\Gamma(\beta-k+1) \Gamma(\beta-n+m-k+1)} & t > 1, \\ \Gamma(n-m+1) \frac{\Gamma(\beta-n+m-1)}{\Gamma(\beta)} & t = 1, \\ 1 & t = 0. \end{cases} \quad (12)$$

$$\kappa_h(\beta, t) = \begin{cases} \prod_{k=1}^t \Gamma(k) \Gamma(n-m-\beta+k) & t > 0, \\ 1 & t = 0. \end{cases} \quad (13)$$

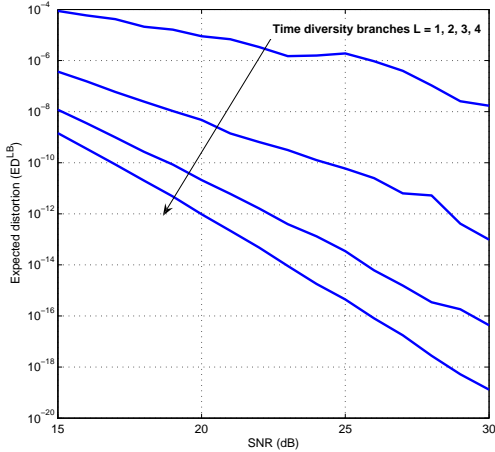


Fig. 2. Expected distortion lower bound at low SCBR. $M = 2$, $N = 1$, $\eta = 0.25$, and $P_s = 1$.

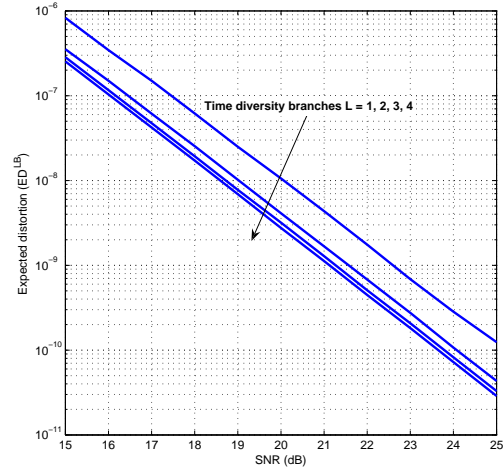


Fig. 3. Expected distortion lower bound at high SCBR. $M = 2$, $N = 4$, $\eta = 1$, and $P_s = 1$.

2, we can see, increasing L decreases ED^{LB} and increases the slope which corresponds to the increase of Δ^{UB} .

When $L > \lceil \frac{2}{\eta(n-m+1)} \rceil$, i.e., $\eta > \frac{2}{L(n-m+1)}$, the system is at high SCBR. In this case, Δ^{UB} is fixed to $2m/\eta$ and thereby has nothing to do with time diversity branches. Then, let us study the behavior of μ^* with L .

The expression (18) can be written as

$$\mu^* = P_s M^{\frac{2m}{\eta}} \left(\prod_{k=1}^m \frac{\Gamma(n-m-\frac{2}{\eta L}+k)}{\Gamma(n-m+k)} \right)^L. \quad (26)$$

Let

$$\varphi(L) = \prod_{k=1}^m \frac{\Gamma(n-m-\frac{2}{\eta L}+k)}{\Gamma(n-m+k)}. \quad (27)$$

It is easy to see $\varphi(L) < 1$ and $\frac{d}{dL}\varphi(L) > 0$. Thus, the derivative of the μ^* with respect to L

$$\frac{d}{dL}\mu^* = P_s M^{\frac{2m}{\eta}} \varphi(L)^L \ln \varphi(L) \cdot \frac{d}{dL}\varphi(L) < 0. \quad (28)$$

Consequently, the corresponding distortion factor μ^* decreases with L at high SCBR and thereby ED^{LB*} also decreases.

Fig.3 shows the relevance between ED^{LB} and L at high SCBR. ED^{LB} 's are figured out by generating 100 000 realizations of \mathbf{H} . We can see that increasing L decreases ED^{LB} but does not change the slope. It corresponds to our analysis

that at high SCBR, increasing L only decreases μ^* and has nothing to do with Δ^{UB} .

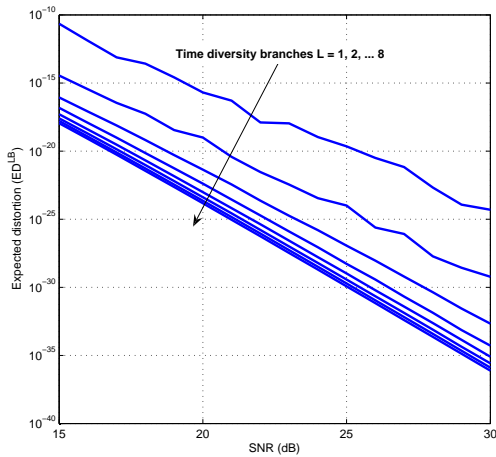
For a system at low SCBR, if we increase L continuously, as indicated by Theorem 3, the SCBR state would transit from *low* to *moderate* and then to *high*. We term the point of L where the systems transits from the moderate SCBR state to the high SCBR state as *transit point*, which is

$$L^* = \lceil \frac{2}{\eta(n-m+1)} \rceil. \quad (29)$$

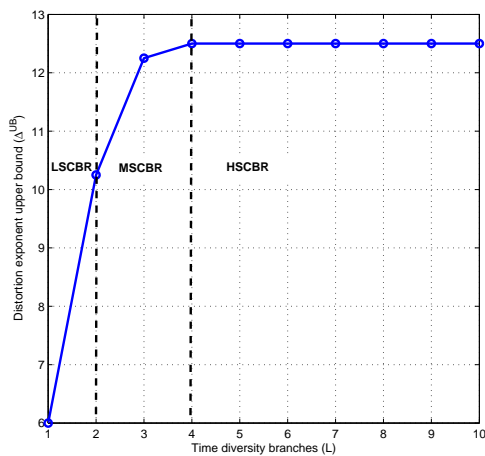
Fig.4 illustrates the transition process. We use Fig.4(b) and Fig. 4(c) to give a theoretical analysis on Fig. 4(a). In Fig.4(b) and Fig. 4(c), the ranges of low, moderate and high SCBRs are denoted by LSCBR, MSCBR and HSCBR, respectively. The transit point L^* in this case is 4. We can see that ED^{LB} decreases with L , but after L^* , because increasing L only affects μ^* , the benefit of increasing L becomes insignificant.

VI. CONCLUSION

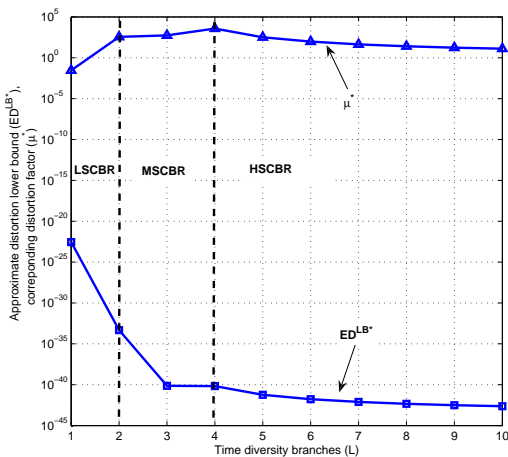
Considering transmitting a white thermal noise source over a time-variant Rayleigh fading MIMO channel, we derived the analytical lower bound of the expected end-to-end distortion, ED^{LB} . It is tight for a no-outage system and loose for an outage-possible system. On the basis of it, we derived the distortion exponent upper bound Δ^{UB} and the corresponding



(a) Expected distortion lower bound



(b) Distortion exponent upper bound



(c) Corresponding distortion factor and approximate expected distortion lower bound at 35 dB SNR

Fig. 4. SCBR state transition with time diversity branches. $M = 2$, $N = 3$, $\eta = 0.32$, and $P_s = 1$.

distortion factor μ^* of the asymptotic ED^{LB*} at high SNR. By studying their behaviors with time diversity branches L , we illustrate that ED^{LB} at high SNR decrease with L . However, when L is larger than the transit point L^* , the system does not benefit much on distortion via increasing L . Therefore, considering the cost of complexity to cope with long frames, when $L > L^*$, we do not suggest lengthen frames to increase L in one frame for the little extra time diversity gain on reproduced source.

REFERENCES

- [1] D. Tse and P. Viswanath, *Fundamentals of Wireless Communication*. Cambridge University Press, 2004.
- [2] S. G. Wilson and Y. S. Leung, "Trellis-coded phase modulation on Rayleigh channels," in *Proc. IEEE Int. Conf. on Communication*, Jun. 1987.
- [3] D. Divsalar and M. K. Simon, "The design of trellis coded modulation for mpsk for fading channels: performance criteria," *IEEE Trans. Commun.*, vol. 36, pp. 1004–1012, Sep. 1988.
- [4] E. Zehavi, "8-psk trellis codes for a Rayleigh channel," *IEEE Trans. Commun.*, vol. 40, pp. 873–884, May 1992.
- [5] J. V-Traveset, G. Caire, E. Biglieri, and G. Taricco, "Impact of diversity reception on fading channels with coded modulation - part: coherent detection," *IEEE Trans. Commun.*, vol. 45, pp. 563–572, May 1997.
- [6] G. Caire, G. Taricco, and E. Biglieri, "Bit-interleaved coded modulation," *IEEE Trans. Inf. Theory*, vol. 44, pp. 927–946, May 1998.
- [7] A. Martinez, A. Guillén, and G. Caire, "Error probability analysis of bit-interleaved coded modulation," *IEEE Trans. Inf. Theory*, vol. 52, pp. 262–271, Jan 2006.
- [8] E. Biglieri, J. Proakis, and S. S. (Shitz), "Fading channels: information-theoretic and communications aspects," *IEEE Trans. Inf. Theory*, vol. 44, pp. 2619–2692, Oct. 1998.
- [9] N. Phamdo and U. Mittal, "A joint source-channel speech coder using hybrid digital-analog(HDA) modulation," *IEEE Trans. Inf. Theory*, vol. 10, pp. 222–231, May. 2002.
- [10] M. R. McKay and I. B. Collings, "Performance bounds for MIMO bit-interleaved coded modulation with zero-forcing receivers," in *Proc. IEEE Global Telecomm. Conf.*, Dec. 2004.
- [11] J. Baltersee, G. Fock, and H. Meyr, "Achievable rate of MIMO channels with data-aided channel estimation and perfect interleaving," *IEEE J. Sel. Areas Commun.*, vol. 19, pp. 2358–2367, Dec 2001.
- [12] C. E. Shannon, "Communication in the presence of noise," *Proc. IRE.*, 1949.
- [13] J. N. Laneman, E. Martinian, G. W. Wornell, and J. G. Apostolopoulos, "Source-channel diversity for parallel channels," *IEEE Trans. Inf. Theory*, vol. 51, pp. 3518–3539, Oct. 2005.
- [14] T. Holliday and A. Goldsmith, "Optimizing end-to-end distortion in MIMO system," in *Proc. IEEE Int. Symp. on Information Theory*, Adelaide, Australia, Sep. 2005.
- [15] G. Caire and K. R. Narayanan, "On the distortion snr exponent of hybrid digital-analog space-time coding," *IEEE Trans. Inf. Theory*, vol. 53, pp. 2867–2878, Aug. 2007.
- [16] D. Gunduz and E. Erkip, "Distortion exponent of MIMO fading channels," in *Proc. IEEE Information Theory Workshop.*, Punta del Este, Uruguay, Mar. 2006.
- [17] L. Zheng and D. N. C. Tse, "Diversity and multiplexing: A fundamental tradeoff in multiple-antenna channels," *IEEE Trans. Inf. Theory*, vol. 49, pp. 1073–1096, May. 2003.
- [18] J. Chen and D. T. M. Slock, "Bounds on optimal end-to-end distortion of mimo links," in *Proc. IEEE Int. Conf. on Communication*, Beijing, China, May. 2008.
- [19] D. Gunduz and E. Erkip, "Joint source-channel codes for MIMO block-fading channels," *IEEE Trans. Inf. Theory*, vol. 10, pp. 116–134, Jan. 2008.
- [20] T. M. Cover and J. A. Thomas, *Elements of Information Theory*. United States: John Wiley & Sons, 1991.
- [21] M. Chiani, M. Z. Win, and A. Zanella, "On the capacity of spatially correlated mimo Rayleigh-fading channels," *IEEE Trans. Inf. Theory*, vol. 49, pp. 2363–2371, Oct. 2003.
- [22] H. Bateman, *Higher Transcendental Functions*. United States: Robert E. Krieger Publishing Company, 1953.